Lunar surface age determination using Chandrayaan-1 TMC data

A. S. Arya*, R. P. Rajasekhar, Guneshwar Thangjam, Ashwin Gujrati, Amitabh, Sunanda Trivedi, B. Gopala Krishna, Ajai and A. S. Kiran Kumar

Space Applications Centre, Indian Space Research Organization, Ahmedabad 380 015, India

Surface age determination is quintessential for understanding and to reconstruct the geo-chronology of any planetary body. The chronology and stratigraphic reconstruction of terrestrial rocks is accomplished by way of radiometric dating, index fossils, litho-stratigraphic correlation, etc. However, in the case of remote planetary bodies, with little accessibility to their rock samples, the Crater Size Frequency Distribution (CSFD) is a well developed method for determining surface ages using remote sensing techniques. India's moon mission, Chandrayaan-I carried a Terrain Mapping Camera (TMC) having high spatial resolution (5 m) and stereo viewing. In the present study, the TMC datasets have been utilized for lunar surface age dating using CSFD and comparing with the radiometrically derived ages of the samples returned by Apollo missions, followed by extension of the same technique for other mare basins, the Copernicus crater and correlating the cratering events in the Taurus–Littrow valley with the Tycho event.

Keywords: Age determination, crater size frequency distribution, lunar surface, terrain mapping camera.

AGE determination of rocks and surface materials for any planetary body is essential for understanding the sequence of geological events in the past and in order to integrate geological units into a stratigraphic column, applicable over the entire planet and to calibrate this column with absolute ages. In case of the Earth, chronology and stratigraphic reconstruction of terrestrial rocks and other materials is accomplished by way of radiometric dating, index fossil, litho-stratigraphic correlation, etc. This involves laboratory analysis of hand specimens/ samples and detailed field study. However, in the case of planetary bodies like the Moon, Mars and asteroids, it becomes challenging to accomplish this task due to insufficient rock samples for carrying out age determination of each part of the planetary body. Planetary surface age determination method, mostly referred to as Crater Size Frequency Distribution (CSFD) method, has wide application due to the presence of impact craters which are the dominant landforms on most of the solid surfaces in our solar system. These impact craters act as a tool to understand the geological history and various surfaces on different planets to reveal spatial and temporal variations of the crater-forming projectile flux as a function of time. The Moon is such a natural laboratory in the entire solar system, which would reveal the history of the inner solar system so as to understand many basic scientific key issues, not only of the Moon, but also of the entire solar system. India's maiden planetary mission to the Moon – Chandrayaan-I, was launched on 22 October 2008. It carried 11 different payloads. One of the sensors, the Terrain Mapping Camera (TMC) had a high spatial resolution of 5 m, stereo-viewing capability in the panchromatic spectral range of 0.5–0.75 μm, and altitude data of 12 bit digitization[1]. The TMC imaged in push-broom mode of 20 km swath in the panchromatic spectral band of 0.5–0.75 μm with a stereo view in the fore, nadir and aft directions of the spacecraft movement and had a base-to-height ratio of 1. The TMC was intended for systematic topographic mapping of the entire lunar surface, including the far side and the polar regions with an aim to prepare a three-dimensional atlas of the Moon with high spatial and altitude sampling for scientific studies. The ortho-image and digital elevation model generated from its stereo pair enable a better study of the morphology of various lunar features.

Impact craters, the dominant landforms on most of the solid surfaces in our solar system, yield footprints of small-body evolution and solar system chronology. Planetary cratering records show a picture of bombardment integrated through the whole geological lifetime of the surfaces studied. Astronomical observations give a snapshot of the small-body population. Planetary geologists can compare surfaces of various ages on different planets to reveal spatial and temporal variations of the crater-forming projectile flux[2]. The number of craters on a surface increases and the crater diameter reduces with the length of time that the surface has been exposed to space. Older surfaces will have more impact craters than younger surfaces, e.g. most Eratosthenian craters were formed with a flux 3–5 times above the modern one, whereas Copernican craters were formed in the last 1–1.5 Ga and reflect the same cratering flux as we have now on the Moon[2]. However, the accuracy of the technique largely depends on our assumptions on scaling laws, nature of crater-forming projectiles, the impact rate difference, etc. These rather simple ideas are the basis for a powerful tool that planetary scientists use to unravel the geological history of a planetary surface.

In the present study, the TMC datasets have been used for crater counting and crater diameter measurements for age dating using the CSFD technique, applied to different surfaces of varying geological ages on the Moon. The results were validated with the radiometric age dating results of the samples from Apollo landing sites and applied to the Imbrium basin, Nubium basin, Copernicus

*For correspondence. (e-mail: arya_as@sac.isro.gov.in)

crater and correlating the central cluster region within the Taurus–Littrow valley with the Tycho event.

Four methods have been used to derive the age of planetary surfaces, i.e. radiometric study of lunar samples[3], studies of crater degradation stage[4], stratigraphic approach[5] and CSFD measurement[6–12].

Radiometric study of lunar sample rocks in the laboratory is restricted to a relatively small number of returned samples and provide ages only at close vicinity of the Luna and Apollo stations. Data derived from crater degradation stages can give us the ages of the entire lunar surface, but numerous endogenic and exogenic processes can influence the appearance of lunar impact craters, decreasing the certainty of age estimation. Ejecta blanket of the impact crater as a stratigraphic marker enabled us to reconstruct a moon wide relative stratigraphy. This provides relative age of the entire lunar surface.

CSFD is widely accepted and used for finding absolute model ages for the lunar surface as well as in other planetary bodies. In using CSFD as a dating tool, two key assumptions were made, i.e. crater formation is a geographically random process and processes destroying the craters operate much slower than the crater-forming processes. For application of CSFD measurement, two steps have to be carried out, i.e. measurement of the surface area of the unit and measurement of crater diameter within each primary lithological unit.

Lunar crater distribution measured on geological units of different ages and in overlapping crater diameter range can be aligned along a complex continuous curve, the lunar production function, by shifting it in $\log N_{\text{cum}}$, i.e. the vertical direction. The lunar production function can be described by 11th polynomial:

$$\log(N_{\text{cum}}) = a_0 + \sum_{k=1}^{11} a_k [\log(D)]^k .$$

The term a_0 represents the time during which a geological unit was exposed to meteorite bombardment. The cumulative crater densities of the geological unit, taken as a fixed reference diameter, are directly related to the time that the units were exposed to the meteorite flux and therefore represent the relative age differences of these units. Relative ages or crater retention ages are obtained by a least square fit of the lunar production function to the actually measured crater distribution, giving the cumulative crater density at the reference diameter.

To obtain absolute model ages from CSFD, the impact rate and its variation through geological time has to be known from returned samples correlated with the crater retention age. Such a correlation of radiometric ages and crater retention ages also allows deriving and calibrating the impact rate on the Moon as a function of time. The lunar crater chronology was established by correlating these radiometric ages with the result from crater count for the landing sites. For this purpose, crater counts for the Apollo 11, 12, 14, 15, 16, 17, and the Luna 16, 24

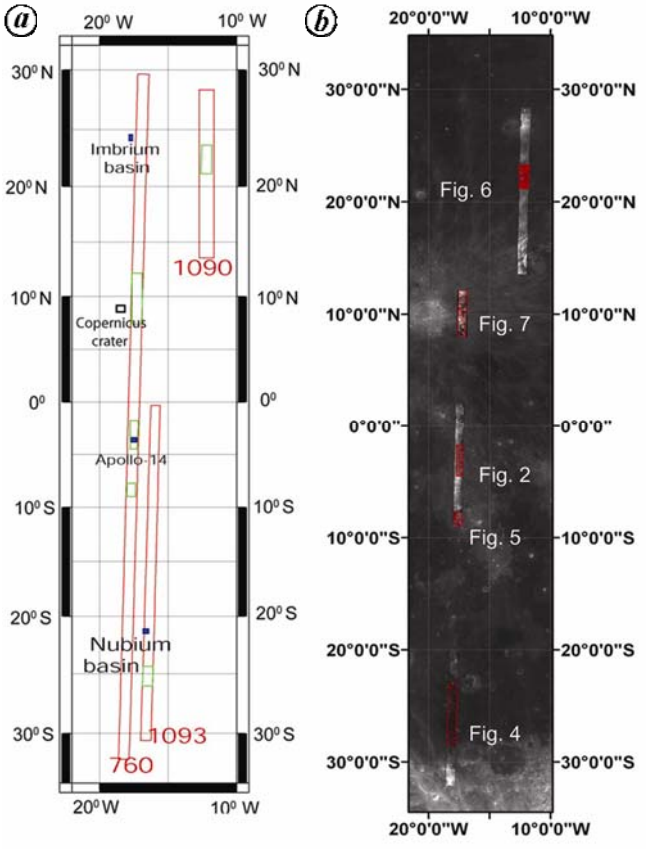

Figure 1. ***a***, Tracks of selected Terrain Mapping Camera (TMC) orbits. ***b***, TMC images showing the study areas (red) superimposed on the Clementine image.

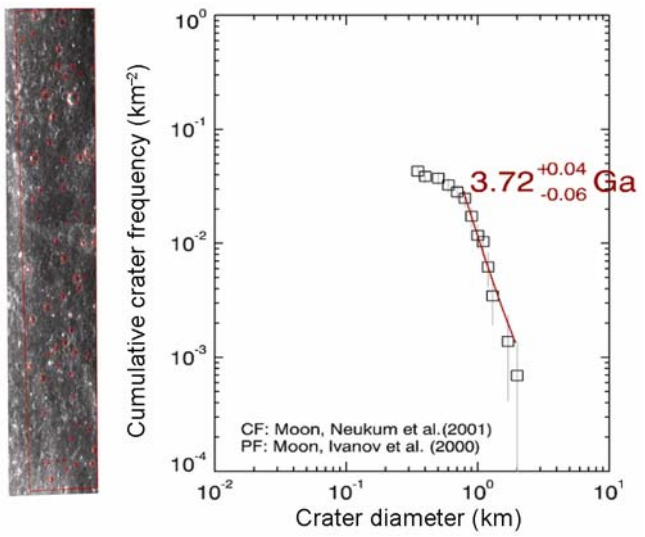

Figure 2. Ortho-image of the Apollo 14 landing site (left) and cumulative Crater Size Frequency Distribution of the counted craters for the selected area (right).The model gives an age of 3.72 Ga.

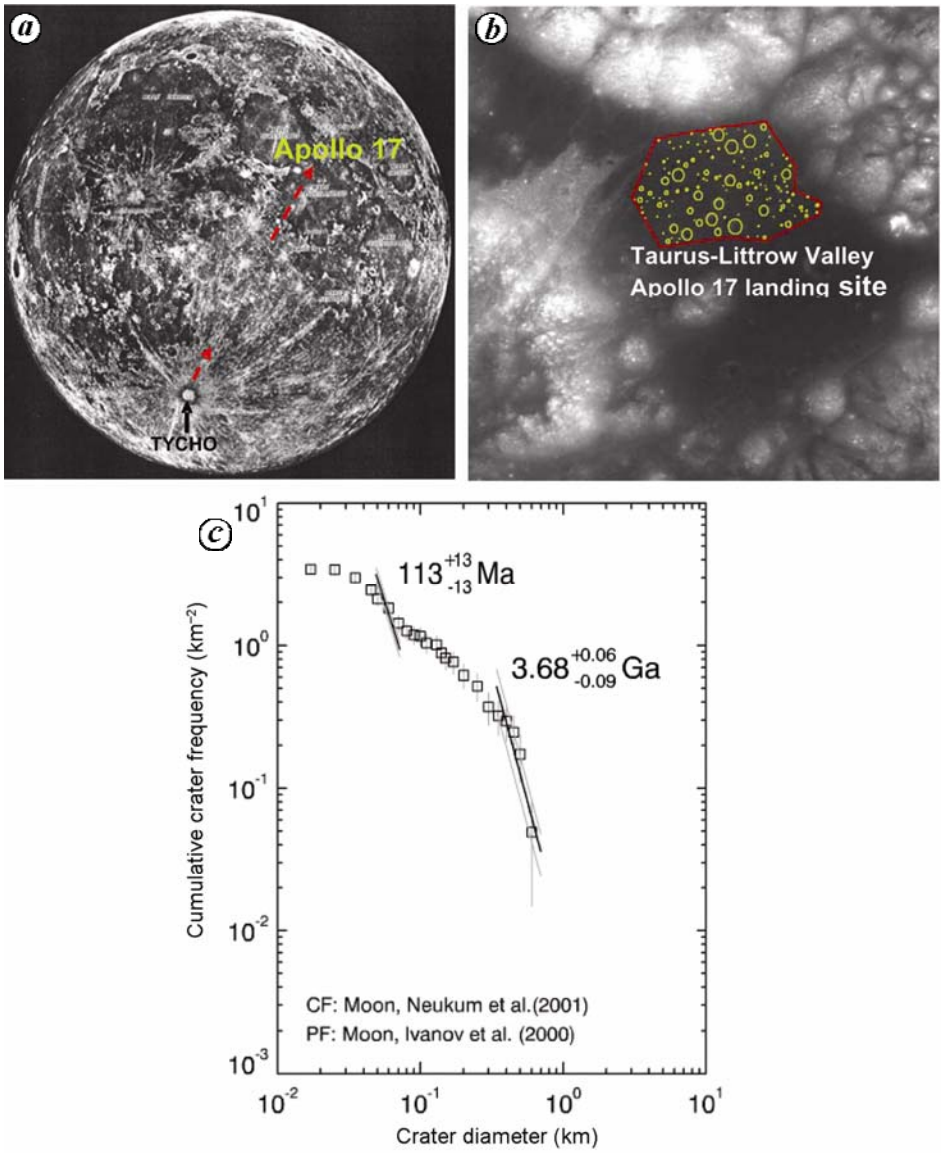

Figure 3. ***a***, Lunar near side showing one of the projectile rays of the Tycho crater extending up to the Apollo 17 landing site. ***b***, Close-up TMC ortho-image of the Apollo 17 landing site/central cluster region in the Taurus–Littrow valley (TLV) considered for age determination using crater counting technique. ***c***, Cumulative CSFD of central cluster region in TLV showing mare age of 3.68 Ga and a resurfaced mare age of 113 Ma, that matches with the age of the Tycho crater.

landing sites were performed and correlated with the corresponding radiometric ages of the sites[6].

The empirically derived lunar impact chronology curve is a least square fit to the available data points and it is mathematically represented by

$$N_{\text{cum}}\ (D \geq 1\ \text{km}) = 5.44 \times 10^{-14}\ [e^{6.93t} - 1] + 8.38 \times 10^{-4} t.$$

An absolute age is derived by solving the above equation for time t for N_{cum} ($D \geq 10$ m) measured on the geological unit.

The method of crater size frequency measurement is generally dependent on quality, i.e. the spatial resolution and illumination conditions of the images on which the crater counts are performed. Contrast, brightness and resolution of the images for crater counts are important issues.

Potential errors in the determination of relative ages with CSFD measurement can be caused by several factors such as flooding, blanketing, secondary cratering, superposition, infilling, abrasion, mass wasting, volcanic crater, etc.

Errors in crater size due to different target materials are irrelevant because as we date only the lunar surface, it is reasonable to assume that the physical properties that might influence the crater size are similar for these entire surface. The level of uncertainty of the crater retention

age for a given count can be calculated using the following formula

$$\pm \sigma N = \log[\{N(1) \pm \sqrt{N(1)}\}/A],$$

where $N(1)$ is the crater retention age calculated for craters of 1 km diameter and A is the size of the counted area. The $\pm \sigma N$ value gives the upper and lower limits of the error bar of the crater retention age.

To obtain reliable ages of surface units with the method of CSFD require certain prerequisites such as mapping of homogeneous units, identification of older craters underlying the substrate, analysis of the erosion state of the surface, elimination of secondary craters and determination of the size of the studied surface area and crater diameter as precisely as possible. In this study, few specific sites were selected so that the area should fall in a homogeneous unit. We assumed that the basalts within a unit are of similar composition and that they represent one large flow unit that may have been derived from a single large or multiple, more or less contemporary smaller eruptions from similar sources.

TMC data were used for surface age determination through CSFD technique applied to Apollo 14 and 17 landing sites. The results were validated by a comparison with the ages of the returned samples. The same was applied to other parts of the lunar surface having different geological ages, and their ages were also determined.

The study area includes landing sites of Apollo 14 and 17 and their vicinity, Imbrium basin centred at 32.8°N lat. and 15.6°W and Nubium basin centred at 21.3°S lat. and 16.6°W long. TMC ortho-image and nadir images having orbit numbers 760, 1090, 1093, acquired at an orbital height of 100 km and swath 20 km on 10 January 2009 were used.

For age determination, homogeneous geological units were selected by overlaying these areas on the regional lunar geological map[5].

The three TMC orbits selected for the study and their location on the Clementine image are shown in Figure 1. Figure 1 *b* also shows the synoptical view of the regional surface features around the selected study areas.

The age of the area surrounding Apollo 14 landing sites was determined using crater counting technique. The crater diameters were measured as precisely as possible from the TMC orthoimages. For the selected area around Apollo 14, an age of 3.72 Ga was obtained (Figure 2). It falls in the upper Imbrian system, which coincides approximately with the age of the returned samples, 3.8–3.9 Ga (ref. 13). This validates our technique and assumptions about age determination using TMC data for this site. Similarly, we calculated the age of the Apollo 17 landing site, whose return sample age is 3.7–3.8 Ga. This is in agreement with the age derived using CSFD technique, i.e. 3.68 Ga with permissible age range (+0.17 to –0.08), as permitted in the dating model (Figure 3). An interesting study was also attempted in the backdrop of a popular belief that projectiles from the Tycho crater had reached the Taurus–Littrow (TL) valley, about 2200 km away. The age of the Tycho crater is about 110–118 Ma (ref. 14) and the crater count of the central cluster in the TL valley furnished an age of about 113 Ma, which indicates that these craters are the footprints of the projectiles from the Tycho crater, thus supporting the popular belief. Figure 3 *a* shows the location of the Tycho crater and the Apollo 17 landing site on the Moon, including the projectile track (a ray) extending from the former to the latter. Figure 3 *b* shows the central cluster regions in the TL valley. Figure 3 *c* shows the CSFD curve of the central cluster and surrounding area within the TL valley. The age of the valley is estimated to be 3.68 Ga, whereas the age of the central cluster region is about 113 Ma, which matches with the age of the Tycho crater.

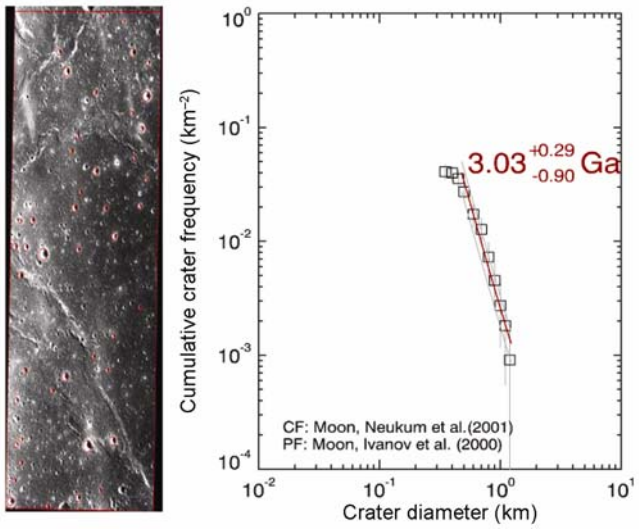

Figure 4. Ortho-image of a part of the Nubium basin, considered for age determination using crater counting technique (left) and cumulative CSFD plot (right). The model gives an age of 3.03 Ga for the area.

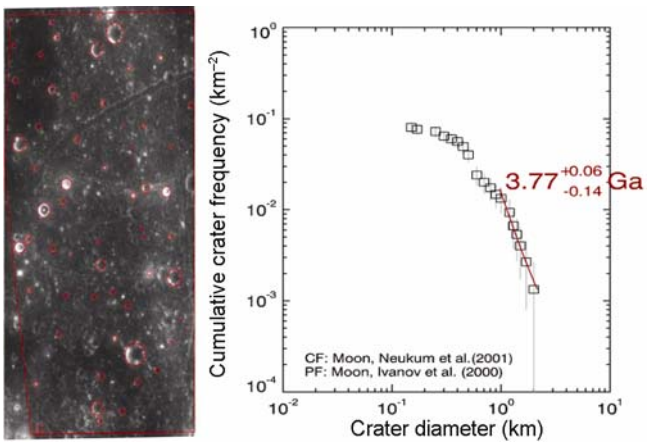

Figure 5. Ortho-image of the area south of Apollo 14 site considered for age determination using crater counting technique (left) and the cumulative CSFD plot (right). The model gives age of 3.77 Ga for the area.

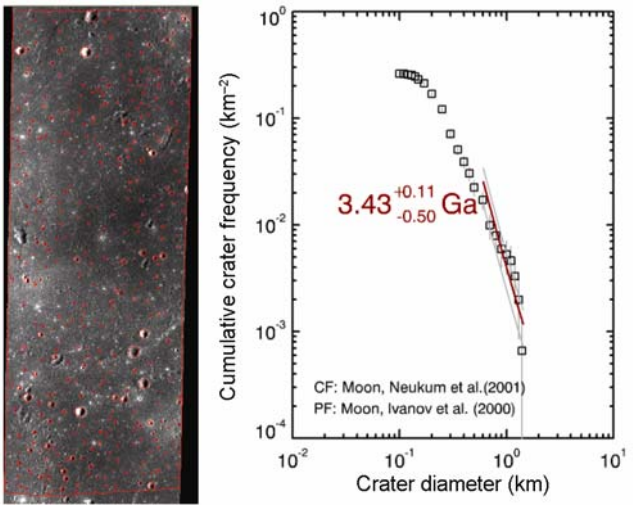

Figure 6. Ortho-image of a part of the Imbrium basin, considered for age determination using crater counting technique (left) and cumulative CSFD plot (right). The model gives age of 3.43 Ga for the area.

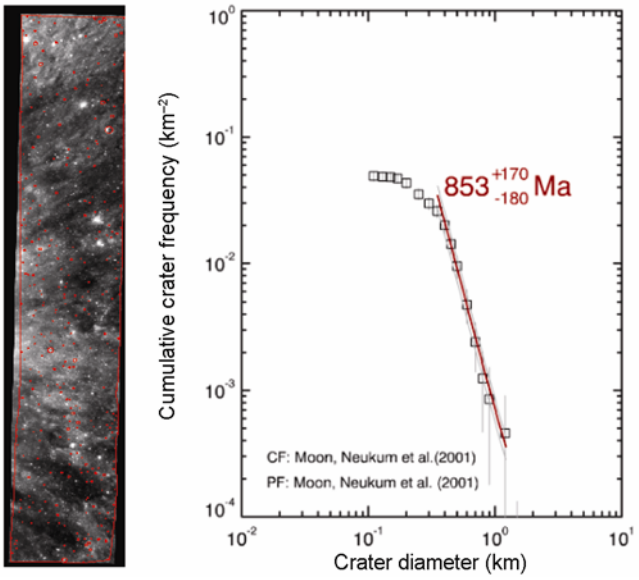

Figure 7. Ortho-image of the Copernicus crater site considered for age determination using crater counting technique (left) and cumulative CSFD plot (right). The model gives age of 853 Ma, which matches with the Copernican age.

After validating the approach, the study was extended to different mare regions in various basins having different geological ages and significance, applying the same methodology and technique. CSFD plots were used to get the best fit so as to give the ages as accurately as possible for each study area. Figure 4 shows the ortho-image of a part of the Nubium basin and the CSFD plot gives an age of 3.03 Ga, which is an Eratosthenian age. The image in Figure 5 is towards south of the Apollo 14 landing site and the CSFD plot give an age of 3.77 Ga, which is an Imbrian age. The image in Figure 6, is a part of Imbrium basin and the CSFD plot gives an age of 3.43 Ga, which is an Imbrian age. The image in Figure 7 is towards west of the Copernicus crater and the CSFD plot gives an age of 853 Ma, which is a Copernican age.

Craters of smaller diameters up to a few metres could be successfully mapped using high-resolution Chandrayaan-I TMC data with high spatial resolution (5 m), which have been used for precise age determination of the lunar surface using crater counting technique.

The technique was successfully validated by applying it to Apollo 14 and 17 landing sites, and the age obtained through CSFD technique matches with that obtained from radiometric dating of the returned samples as well as with the earlier reported results. This technique was further extended to south of the Apollo 14 landing site, Imbrium basin, Nubium basin and east of the Copernicus crater. The corresponding ages obtained using this technique were 3.77 Ga, 3.43 Ga, 3.02 Ga, 895 Ma respectively, which are in good agreement with the earlier reported ages. Thus, the TMC data have shown application in lunar surface age determination through remote sensing technique (CSFD) as well as for correlating different geological events.

1. Kiran Kumar, A. S. *et al.*, Terrain Mapping Camera: A stereoscopic high-resolution instrument on Chandrayaan-1. *Curr. Sci.*, 2009, **96**, 492–495.
2. Neukum, G., Ivanov, B. A. and Hartmann, W. K., Cratering records in the inner solar system in relation to the lunar reference system. *Space Sci. Rev.*, 2001, **96**, 55–86.
3. Basaltic Volcanism Study Project, *Basaltic Volcanism on the Terrestrial Planets*, Pergamon, New York, 1981, p. 1286.
4. Boyce, J. M., Ages of flow units in the lunar nearside maria based on Lunar Orbiter IV photographs. In Proceedings of 7th Lunar Science Conference, Houston, Texas, 15–19 March 1976, pp. 2717–2728.
5. Wilhelms, D. E. *et al.*, The geologic history of the Moon. U.S. Geol. Surv. Prof. Pap., 1987, 1348, pp. 302.
6. Hiesinger, H., Jaumann, R., Neukum, G. and Head, J. W., Ages of mare basalts on the lunar nearside. *J. Geophys. Res.*, 2000, **105**, 29,239–29,275.
7. Neukum, G., Ivanov, B. A. and Hartmann, W. K., Cratering records in the inner solar system in relation to the lunar reference system. *Space Sci. Rev.*, 2001, **96**, 55–86.
8. Ivanov, B. A., Mars/moon cratering rate ratio estimates. *Space Sci. Rev.*, 2001, **96**, 87–104.
9. Michael, G. G. and Neukum, G., Planetary surface dating from crater size–frequency distribution measurements; partial resurfacing events and statistical age uncertainty. *Earth Planet Sci. Lett.*, 2010, **294**, 223–229; doi: 10.1016/j.epsl.2009.12.041
10. Neukum, G. and Ivanov, B. A., Crater size distributions and impact probabilities on earth from lunar, terrestrial-planet, and asteroid cratering data. In *Hazard Due to Comets and Asteroids*, Univ. of Ariz. Press, Tucson, USA, 1994, pp. 359–416.
11. Haruyama, J. *et al.*, Long-lived volcanism on the lunar farside revealed by SELENE terrain camera. *Science*, 2009, **905**, 323; DOI: 10.1126/science.1163382.
12. Shylaja, B. S., Determination of lunar surface ages from crater size frequency distribution. *J. Earth Syst. Sci.*, 2005, **114**(6), 609–612; DOI: 10.1007/BF02715944.

13. Spudis, P. and Pieters, C., Global and regional data about the moon. In *Lunar Sourcebook*, Cambridge University Press, 1991, pp. 610.
14. Heisinger, H. *et al.*, New crater size-frequency distribution measurements for Tycho crater based on lunar reconnaissance orbiter camera images, In 41st Lunar and Planetary Science Conference, Houston, Texas, 2010, Abstract # 2287.

ACKNOWLEDGEMENTS. We thank Dr R. R. Navalgund, Director, Space Applications Centre (SAC), for encouragement; Dr J. S. Parihar, DD-EPSA/SAC, Ahmedabad for guidance, and Greg Michael, Freie Universiat, Berlin, for help and suggestions while implementing CSFD. We also thank Dr B. S. Shylaja, Jawaharlal Nehru Planetarium, Bangalore and Thomas Kniessl, Freie Universitat, Berlin, for help.

Received 21 December 2011; accepted 30 January 2012

Tectonic implications of the September 2011 Sikkim earthquake and its aftershocks

M. Ravi Kumar[1,*], Pinki Hazarika[1], G. Srihari Prasad[1], Arun Singh[2] and Satish Saha[1]

[1]National Geophysical Research Institute (CSIR), Hyderabad 500 007, India
[2]Department of Geology and Geophysics, Indian Institute of Technology, Kharagpur 721 302, India

This study presents results of the spatial patterns of 292 aftershocks of the *Mw* 6.9 Sikkim earthquake of September 2011, accurately located through analysis of three component waveforms registered by a five station broadband network operated immediately after its occurrence. Refined hypocentral parameters achieved through application of the hypoDD relocation scheme reveal tight clustering of events along a NW–SE trend with focal depths reaching ~60 km. These trends viewed in conjunction with the strike–slip mechanisms of past earthquakes in Sikkim, including the main shock, affirm the predominance of transverse tectonics in this segment of the Himalaya where the Indian plate convergence seems to be accommodated by dextral motion along steeply dipping fault systems.

Keywords: Aftershocks, earthquakes, hypocentral parameters, spatial patterns, transverse tectonics.

THE devastating *Mw* 6.9 earthquake that occurred to the northwest of Sikkim on 18 September 2011, presents a fresh opportunity to reassess the seismotectonics of this intriguing segment of the Himalaya, which otherwise presents a classic example of continental collision. The epicentre of this earthquake, which claimed at least 100 lives, is located near the border between India and Nepal, at 27.72°N and 88.14°E, with a focal depth[1] of about 50 km. A preliminary account of this earthquake, including description of the damage to the landscape and engineering structures, the seismotectonic scenario, and discrepancies in the hypocentral locations reported by various agencies, is succinctly summarized in a recent paper[2]. The strike–slip nature of the 2011 Sikkim earthquake (Figure 1) reiterates the dominance of transverse tectonics in the regions of Sikkim and Bhutan[3,4], in contrast to a thrust environment in other segments of the Himalaya (Figure 2) manifested as shallow underthrusting of the Indian tectonic plate beneath Eurasia along the plane of detachment coinciding with the Main Himalayan Thrust. Whether the strike–slip motion is associated with the Indian plate or the overriding Himalayan wedge remains contentious in view of the uncertainty in the hypocentral parameters of this earthquake, although knowledge of the accurate geometry, fine structure and thickness of the crust in the Sikkim and adjacent Nepal Himalaya exists from receiver function studies[5,6]. Also, given the earthquake focal mechanism, even to a high degree of accuracy, the implicit ambiguity in choosing the true fault plane imposes constraints on identifying the causative tectonic features apparent on the surface or concealed within the subsurface. For instance, considering the NE–SW plane as the true fault plane of the 2011 Sikkim earthquake and the *M* 6.6 Udaipur earthquake of 20 August 1988, which had a similar focal mechanisms, it was suggested that these earthquakes occurred in response to the subducting Munger–Sahasra ridge under the Himalayan arc[7]. On the contrary, if the NW–SE plane is the true plane, dextral motion along steeply dipping lineaments like Gantok and Tista would be accommodating the Indian plate convergence, assuming that these lineaments extend to lower crustal/upper mantle depths[3,4]. Study of the spatial distribution of aftershocks is, therefore, the ideal way to resolve the fault plane ambiguity and identify the causative faults, since these shocks would occur on the fault plane in response to slip due to the main shock.

Akin to the rest of the Himalaya, the Main Boundary Thrust (MBT) and the Main Central Thrust (MCT) are geologically well expressed in Sikkim, albeit a peculiar overturn of the latter. In addition to these, the prominent tectonic features in this province are the two near-parallel, NNW–SSE trending Tista and Gangtok lineaments, the WNW–ESE trending Goalpara lineament and the SW–NE trending Kanchanjangha fault (Figure 3). Previous seismicity studies in the region using data from local networks, reveal that the epicentres are mainly confined between MBT and MCT[4,8]. However, the recent earthquake appears to have occurred further north of these thrust zones, with two of its largest aftershocks (*M* 4.8 and 4.7 on the same day), located SE of the epicentre of the main shock, close to MCT (Figure 3).

*For correspondence. (e-mail: kumar_mr1@rediffmail.com)